Received: 9 June 2021 | Revised: 24 August 2021 | Accepted: 20 September 2021

DOI: 10.1002/eco.2361

RESEARCH ARTICLE

WILEY

MPeat—A fully coupled mechanical-ecohydrological model of peatland development

Adilan W. Mahdiyasa[1,2] | David J. Large[1] | Bagus P. Muljadi[1] | Matteo Icardi[3] | Savvas Triantafyllou[4]

[1]Department of Chemical and Environmental Engineering, University of Nottingham, Nottingham, UK

[2]Department of Mathematics, Bandung Institute of Technology, Bandung, Indonesia

[3]School of Mathematical Sciences, University of Nottingham, Nottingham, UK

[4]Institute for Structural Analysis and Aseismic Research, School of Civil Engineering, National Technical University of Athens, Athens, Greece

Correspondence
Adilan W. Mahdiyasa, Department of Mathematics, Bandung Institute of Technology, Bandung 40132, Indonesia.
Email: adilan.mahdiyasa@nottingham.ac.uk; adilan@math.itb.ac.id

David J. Large, Department of Chemical and Environmental Engineering, University of Nottingham, University Park, Nottingham NG7 2RD, UK.
Email: david.large@nottingham.ac.uk

Funding information
Directorate General of Higher Education

Abstract

Mathematical models of long-term peatland development have been produced to analyse peatland behaviour. However, existing models ignore the mechanical processes that have the potential to provide important feedback. Here, we propose a one-dimensional model, MPeat, that couples mechanical, ecological and hydrological processes via poroelasticity theory, which couples fluid flow and solid deformation. Poroelasticity formulation in the MPeat is divided into two categories, fully saturated and unsaturated. To validate this formulation, we compare numerical solutions of the fully saturated case with analytical solutions of Terzaghi's problem. Two groups of MPeat simulations are run over 6,000 years using constant and variable climate, and the results are compared to those of two other peat growth models, DigiBog and the Holocene Peat Model. Under both climatic conditions, MPeat generates the expected changes in bulk density, active porosity and hydraulic conductivity at the transition from the unsaturated to the saturated zone. The range of values of peat physical properties simulated by MPeat shows good agreement with field measurement, indicating plausible outputs of the proposed model. Compared to the other peat growth models, the results generated by MPeat illustrate the importance of poroelasticity to the behaviour of peatland. In particular, the inclusion of poroelasticity produces shallower water table depth, accumulates greater quantities of carbon and buffers the effect of climate changes on water table depth and carbon accumulation rates. These results illustrate the importance of mechanical feedbacks on peatland ecohydrology and carbon stock resilience.

KEYWORDS
carbon stock, compression, ecohydrology, effective stress, peatland development, poroelasticity

1 | INTRODUCTION

At a fundamental level, the compaction of water-saturated dead organic matter to form peat is a mechanical process. Yet, on account of numerical complexity and possibly strong ecohydrological focus, the previous models of peat growth do not incorporate mechanics. It is the purpose of this paper to present a fully coupled mechanical-ecohydrological model for peat growth and consider the potential implications of feedback within this model system.

Peatlands are complex systems (Belyea, 2009; Belyea & Baird, 2006) with the potential to shift dramatically between equilibrium states in response to environmental change, potentially releasing large quantities of carbon (Jackson et al., 2017; Loisel et al., 2017; Lunt et al., 2019; Yu et al., 2010). One approach to understanding this

complex behaviour is through mathematical models that provide insight into the functioning of the peatland system on a wide range of timeframes and particularly beyond the timeframes of direct observation. These mathematical models of peatland development enable us to analyse nonlinear behaviour because of the internal feedback mechanisms (Hilbert et al., 2000; Morris et al., 2011) and the effects of past or future events on peatland carbon storage, for example, climate change (Heinemeyer et al., 2010; Ise et al., 2008; Yu et al., 2001) or drainage (Young et al., 2017).

The most advanced peatland development models are based on ecohydrological processes. For example, the one-dimensional Holocene Peat Model (HPM) (Frolking et al., 2010) groups peatland vegetation into 12 plant functional types (PFTs) based on their characteristics, the quantities of which are determined by the water table depth and nutrient status. Associated with each PFT is a productivity and a decomposition rate, the balance of which determines rates of peat accumulation. The effect of decomposition is tracked for each peat cohort in terms of the remaining mass, which in turn determines the bulk density, hydraulic conductivity and porosity. DigiBog (Baird et al., 2012; Morris et al., 2011, 2012), a one-, two- or three-dimensional peatland development model, is built on a series of coupled ecological and hydrological processes that are divided into plant litter production, decomposition, hydraulic properties and a hydrological submodel. The hydrological submodel determines water table position and hence litter production and decomposition, which in turn affects hydraulic conductivity. However, bulk density and drainable porosity are held constant. The potential problem with this approach is that HPM, DigiBog and similar models (e.g., Heinemeyer et al., 2010; Hilbert et al., 2000; Swinnen et al., 2019) ignore the mechanical cause of changes in peat physical properties that have the potential to influence the ecohydrology and peatland resilience. Examples of such mechanical effects that cannot be captured in these models include variable loading of the peat surface as productivity changes, the motion of the peat surface in response to changes in the height of the water table and mechanical failure of the peat body.

Peat is a mechanically weak, poroelastic material due to its extremely high water content and void ratio with values ranging between 500–2,000% and 7.5–30, respectively (Hanrahan, 1954; Hobbs, 1986, 1987; Mesri & Ajlouni, 2007). As a result, the changes in peat pore structure, which significantly influence hydraulic properties, are not only determined by progressive decomposition (Moore et al., 2005; Quinton et al., 2000) but also compression. Hydraulic conductivity decreases when the water table drops due to the mechanical deformation in the pore structure (Whittington & Price, 2006), an important process that can reduce water discharge from peatland. In a similar way, the enhancement of water input will expand the pore space that leads to an increase in hydraulic conductivity, promoting higher water loss from peatland. Swelling or shrinking of the pore space caused by mechanical deformation leads to the seasonal surface fluctuation, with the magnitude determined by several factors, such as Young's modulus, which is a measure of the stiffness of an elastic material, gas content and loading effects (Glaser et al., 2004; Reeve et al., 2013).

In this paper, we present a new fully coupled one-dimensional mechanical, ecological and hydrological peatland development model. Although the one-dimensional model is clearly a simplification of the real problem, it provides an insight into how our model simulates peatland as a complex system. The overall structure of the paper takes the form of three parts. The first part deals with the model formulation that provides detailed explanations about the governing equations and verification of the numerical method. This part also describes the changes in peat physical properties, including bulk density, active porosity (pores that actively transmit water; Hoag & Price, 1997), hydraulic conductivity and Young's modulus as part of the internal feedback mechanism. The second part presents model implementations and simulation results, which are run under two different cases, constant and non-constant climatic conditions. In the last part, we consider the implications of this model for peatland processes and discuss several aspects that can be developed to produce a more plausible model of peatland development.

Throughout the paper, we use the following precise definitions of the terms compaction, consolidation and compression. Compaction is the reduction in volume due to the decrease in void space through the rearrangement of solid particles. If the volume reduction is caused by the expulsion of excess pore water pressure, it is called consolidation. The term compression refers to the process of applying inward or compressive forces to the material.

2 | MODEL FORMULATION

MPeat is conceptualized as a one-dimensional column of peat at the centre of a peatland with a new layer added every time step. As the peatland develops, its physical properties are affected by the feedback from the mechanical, ecological and hydrological processes through the coupling between fluid flow and solid deformation, which is known as poroelasticity, and this is the essence of our model (Figure 1). Peatland accumulates carbon since peat production from plant litter or organic matter is generally greater than peat decomposition. The rate of decay is high due to the unsaturated aerobic condition above the water table (unsaturated zone). In contrast, the condition is fully saturated below the water table (saturated zone), resulting in a low rate of anaerobic decay. Peat that is more decomposed becomes susceptible to deformation because of the decrease in strength and Young's modulus. This deformation affects the structure of pore space, represented by the change in bulk density, active porosity and hydraulic conductivity. To accommodate this process, we define physical properties functions as follows:

$$\rho = \rho(b,u,z), \tag{1}$$

$$\phi = \phi(b,u,z), \tag{2}$$

$$\kappa = \kappa(\phi), \tag{3}$$

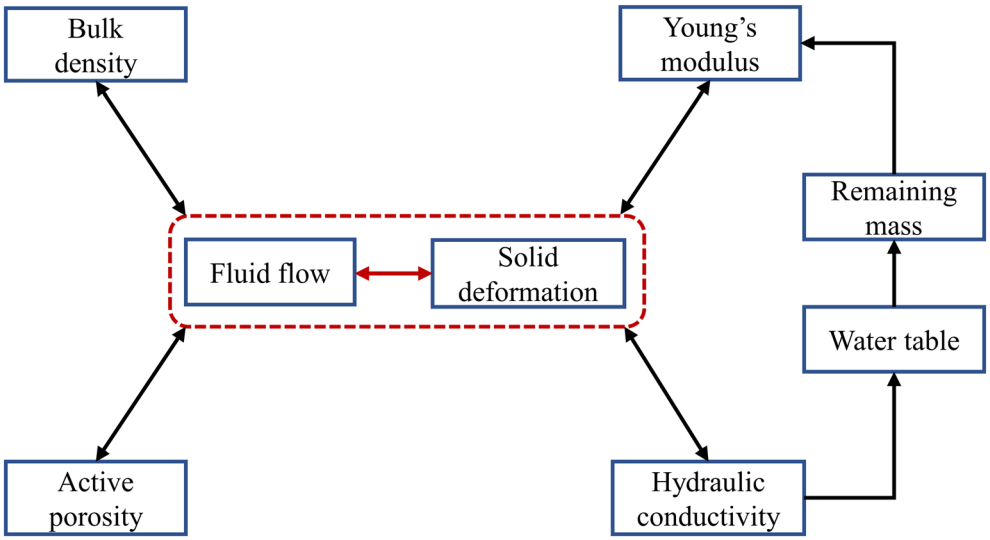

FIGURE 1 Schematic illustration of MPeat explains the interactions between peat physical properties, including bulk density, active porosity, hydraulic conductivity and Young's modulus through the coupling between fluid flow and solid deformation

$$E = E(\theta), \tag{4}$$

where ρ is the bulk density (kg m^{-3}), ϕ is the active porosity (–), κ is the hydraulic conductivity (m s^{-1}), E is the Young's modulus (Pa), b is the peatland height (m), u is the vertical displacement (m), z is the water table depth (m) and θ is the remaining mass (–). MPeat is divided into three submodels, mechanical, ecological and hydrological as explained below.

2.1 | Mechanical submodel

Peat can be viewed as a porous medium because it consists of solid particles from plant litter or organic matter, and the pores are filled with fluid. The total stresses that act on a porous medium are allocated to pore fluid and the solid skeleton. The first component leads to the excess pore fluid pressure, and the second component, termed the effective stress (Terzaghi, 1943), leads to the displacement of the solid. The effective stress is a part of the total stress defined as

$$\sigma' = \sigma - np, \tag{5}$$

where σ' is the effective stress (Pa), σ is the total stress (Pa), n is the effective stress coefficient (–), and p is the excess pore fluid pressure (Pa). The excess pore fluid pressure and the solid displacement can be solved simultaneously through the poroelasticity concept.

The poroelasticity formulation in the mechanical submodel is divided into two categories, that is, fully saturated and unsaturated, to accommodate the peatland characteristics. The fully saturated poroelasticity is developed to analyse the features of the saturated zone and follows Biot's theory of consolidation (Biot, 1941). For the one-dimensional case, the governing equations are explained as follows. The equation of equilibrium without body force has the following form:

$$\frac{\partial \sigma}{\partial y} = 0, \tag{6}$$

where σ is the total stress (Pa). Equation 6 is obtained from Newton's law of motion, stating that in the absence of acceleration, all of the forces acting on a small element of material must balance.

The kinematic relation that links strain and displacement (Equation 7) and the linear constitutive law that gives the relation between effective stress and strain (Equation 8) can be written as

$$\epsilon = \frac{\partial u}{\partial y}, \tag{7}$$

$$\sigma' = E\epsilon, \tag{8}$$

where ϵ is the strain (–), u is the vertical displacement (m), σ' is the effective stress (Pa) and E is the Young's modulus (Pa).

By introducing the conservation of mass of solid particles and water, together with Darcy's law for the flow of water in the porous medium, we can get

$$\alpha \frac{\partial \epsilon}{\partial t} + \frac{1}{M}\frac{\partial p_w}{\partial t} = \kappa \frac{\partial^2 p_w}{\partial y^2}, \tag{9}$$

where α is the Biot's coefficient (–), ϵ is the strain (–), M is the Biot's modulus (Pa), p_w is the excess pore water pressure (Pa) and κ is the hydraulic conductivity (m s^{-1}). The interpretation of Equation 9 is that the compression of a fully saturated porous medium consists of the compression of pore water, solid skeleton and the amount of water expelled from it by the flow. The value of α is equal to one (Terzaghi, 1943), and M is equal to the inverse of the specific storage, that is, $M = \frac{1}{S_s}$ (Cheng, 2020; Green & Wang, 1990). In this formulation, the vertical head gradient is contained in the excess pore water pressure, which in turn influences the effective stress. Furthermore, the

lower boundary is impermeable and experiences no displacement, while the upper boundary is fully drained.

In the unsaturated zone, water and air occupy the pore space. As the depth of the unsaturated zone is usually less than 0.5 m (Ballard et al., 2011; Ingram, 1982; Swinnen et al., 2019), we assume air pressure equal to atmospheric pressure. By making this assumption, Equation 9 can be extended to represent the unsaturated zone as

$$\alpha_w \frac{\partial \epsilon}{\partial t} + \frac{1}{M_w}\frac{\partial p_w}{\partial t} = \kappa \frac{\partial^2 p_w}{\partial y^2}. \tag{10}$$

The parameters α_w and M_w depend on the degree of saturation of water (Cheng, 2020):

$$\alpha_w = S_w, \tag{11}$$

$$M_w = \frac{\gamma_w(1-\lambda)}{\phi\lambda\mu} S_w^{-1/\lambda}\left(1 - S_w^{1/\lambda}\right)^{\lambda}, \tag{12}$$

where S_w is the degree of saturation of water (−), γ_w is the specific weight of water (N m^{-3}), ϕ is the active porosity (−), λ is the first water retention empirical constant (−), μ is the second water retention empirical constant (m^{-1}), ϵ is the strain (−), p_w is the excess pore water pressure (Pa) and κ is the hydraulic conductivity (m s^{-1}).

The mechanical submodel is described in terms of a partial differential equation with two independent variables that are space y and time t, while ecological and hydrological submodels only contain time t as an independent variable on their differential equation. To provide a fully coupled model, the space discretisation in the mechanical submodel is obtained from the layer thickness as follows:

$$h = \frac{m}{\rho}, \tag{13}$$

where h is the layer thickness (m), m is the peat mass per unit area (kg m^{-2}) and ρ is the bulk density (kg m^{-3}).

Mechanical deformation of the peat body cannot be separated from water table depth, peat production and decomposition. Water table depth determines peat production and plant weight at the top surface (see Section 2.2), which have a role as load sources. Besides that, water table depth also influences the effective stress because a deeper water table position leads to higher effective stresses and increases deformation. This process reduces the void space and brings the solid particles into closer contact with one another through vertical displacement, increasing the bulk density and decreasing active porosity

$$\rho_t = \rho_{t-1}\left(\frac{b_{t-1}}{b_{t-1} - u_{t-1}(1+\beta z_{t-1})}\right), \tag{14}$$

$$\phi_t = \phi_{t-1}\left(\frac{b_{t-1} - u_{t-1}(1+\beta z_{t-1})}{b_{t-1}}\right), \tag{15}$$

where ρ is the bulk density (kg m^{-3}), ϕ is the active porosity (−), b is the peatland height (m), u is the vertical displacement (m), β is the bulk density and active porosity parameter (m^{-1}) and z is the water table depth (m). The subscripts indicate the updated value of bulk density and active porosity from the previous time. The other factor that affects mechanical deformation significantly is decomposition. Zhu et al. (2020) showed that the decomposition reduces the strength and Young's modulus of dead roots, one of the main constituents of peat fibre. This result leads us to the conclusion that the Young's modulus should decrease as peat decompose. For the initial model, we propose an equation that includes the effect of decomposition on the peat Young's modulus as a linear function:

$$E_t = \chi\left(1 + \theta_t^{\varsigma}\right), \tag{16}$$

where E is the Young's modulus (Pa), θ is the remaining mass (−), χ is the first Young's modulus parameter (Pa) and ς is the second Young's modulus parameter (−).

2.2 | Ecological submodel

Peat production follows the equation from Morris et al. (2015), which depends not only on the water table depth but also on the air temperature. This equation is the development of Belyea and Clymo (2001) and can be written as

$$\begin{gathered}\psi = 0.001\left(9.3 + 133z - 0.022(100z)^2\right)^2(0.1575Temp + 0.0091), \\ \text{for } 0 \le z \le 0.668 \\ \psi = 0, \\ \text{for } z > 0.668\end{gathered}, \tag{17}$$

where ψ is the peat production (kg m^{-2} year^{-1}), z is the water table depth (m) and *Temp* is the air temperature (°C). Peat production has a strong relationship with above-ground biomass that can be used to model the plant weight at the top surface through the equation and data from Moore et al. (2002). To accommodate the wet condition of the plant that consists of shrub, sedge or herb, and *Sphagnum*, we multiply each type with a constant that is obtained from its water content. Thus, we may write the equation for plant weight

$$\begin{aligned}\Upsilon = c_1\left(10^{\frac{\log_{10}(\psi)+0.409}{0.985}}\right)(1+d_1)g + c_2\left(10^{\log_{10}(\psi)+0.001}\right)(1+d_2)g \\ +(c_3 0.144)(1+d_3)g,\end{aligned} \tag{18}$$

where Υ is the plant weight (Pa); ψ is the peat production (kg m^{-2} year^{-1}); g is the acceleration of gravity (m s^{-2}); c_1,c_2,c_3 are the plant proportions (−) and d_1,d_2,d_3 are the constants for plant wet condition (−) with the indices 1,2,3 indicating shrub, sedge or herb, and *Sphagnum*, respectively. Besides peat production, the accumulation of mass in the peatland is also influenced by the decomposition process. It occurs in both zones, unsaturated and saturated, but at a different

rate. If we assume that the rate of decay is constant at each zone, then the change of mass because of decay can be modelled as (Clymo, 1984)

$$\frac{dm}{dt} = -\eta m, \tag{19}$$

where m is the mass per unit area (kg m^{-2}) and η is the rate of decay (year^{-1}). Furthermore, the quotient between mass at time t, which has experienced decay, and the initial mass gives us the remaining mass of the peat, or formally

$$\theta_t = \frac{m_t}{m_0}, \tag{20}$$

where θ is the remaining mass (–), m_t is the mass per unit area at time t (kg m^{-2}) and m_0 is the initial mass per unit area (kg m^{-2}).

2.3 | Hydrological submodel

The change in active porosity due to compression affects hydraulic conductivity because water cannot move easily as the pore size becomes smaller. Therefore, one of the ways to model the relationship between hydraulic conductivity and active porosity is

$$\kappa_t = \kappa_0 \left(\frac{\phi_t}{\phi_0}\right)^{\xi}, \tag{21}$$

where κ is the hydraulic conductivity (m s^{-1}), κ_0 is the initial value of hydraulic conductivity (m s^{-1}), ϕ is the active porosity (–), ϕ_0 is the initial value of active porosity (–) and ξ is the hydraulic conductivity parameter (–). Because compression is influenced by decomposition through Young's modulus (see Equation 16), we can also interpret hydraulic conductivity in Equation 21 as a function of decay. DigiBog also uses this interpretation to develop its hydrophysical submodel (Baird et al., 2012; Morris et al., 2012).

The water table varies over time in response to the internal and external factors, including change in the active porosity, hydraulic conductivity, peatland radius and net rainfall. We employ the equation from Childs (1969) (see also Swindles et al., 2012) to predict the water table height at the centre of the peatland:

$$\frac{d\Gamma}{dt} = \frac{r}{\phi} - \frac{2\kappa\Gamma^2}{l^2\phi}, \tag{22}$$

where Γ is the water table height (m), r is the net rainfall (m yr^{-1}), l is the peatland radius (m), ϕ is the active porosity (–) and κ is the hydraulic conductivity (m s^{-1}). The difference between peatland height and water table height at time t results in the water table depth of the peatland, or mathematically

$$z = b - \Gamma, \tag{23}$$

where z is the water table depth (m) and b is the peatland height (m). Water table height cannot exceed peatland height because we assume all the water will flow as surface water over the peatland area.

2.4 | Numerical formulation and verification

Poroelasticity is used to couple mechanical, ecological and hydrological submodels through the changes in peat physical properties, including bulk density, active porosity, hydraulic conductivity and Young's modulus. These changes simultaneously affect the calculations from each submodel. Therefore, in the MPeat, each submodel does not run sequentially to obtain the final results.

MPeat ecological and hydrological submodels are solved using the finite difference method, which is similar to Morris et al. (2015) but with two main differences: first, the formulation and assumption to calculate the changes in peat physical properties and, second, the influence of air temperature on the decomposition process (see openly available MPeat simulation codes for detailed numerical formulation).

In this section, we focus on the numerical formulation and verification of MPeat mechanical submodel. We apply the finite element method (see Zienkiewicz et al., 2013) to approximate the solution of the mechanical submodel in which the primary variables are solid displacement and excess pore water pressure. We compare the numerical solution of a fully saturated case (Equations 6–9) with the analytical solution of Terzaghi's problem to validate the finite element algorithm. In this test case, a uniform vertical load q is applied on the top surface of a fully saturated sample with height H. The boundary conditions are the same with mechanical submodel formulation. If the initial value of excess pore water pressure is p_{w0}, then

$$p_w(y,0^+) = p_{w0}, \tag{24}$$

$$\frac{dp_w}{dy} = 0, \text{ at } y = 0, \tag{25}$$

$$u(0,t) = 0, \tag{26}$$

$$p_w(H,t) = 0, \tag{27}$$

where p_w is the excess pore water pressure (Pa) and u is the vertical displacement (m). The excess pore water pressure and vertical displacement are expressed as non-dimensional quantities normalized excess pore water pressure P and degree of consolidation U:

$$P = \frac{p_w(y,t)}{p_{w0}}, \tag{28}$$

$$U = \frac{u(y,t) - u(y,0^+)}{u(y,\infty) - u(y,0^+)}. \tag{29}$$

The analytical solutions of Terzaghi's problem are (Biot, 1941; Verruijt, 2018; Wang, 2000)

$$P = \frac{4}{\pi}\sum_{k=1}^{\infty}\frac{(-1)^{k-1}}{2k-1}\cos\left[(2k-1)\frac{\pi}{2}\frac{y}{H}\right]\exp\left[-(2k-1)^2\frac{\pi^2}{4}\frac{c_v t}{H^2}\right], \quad (30)$$

$$U = 1 - \frac{8}{\pi^2}\sum_{k=1}^{\infty}\frac{1}{(2k-1)^2}\exp\left[-(2k-1)^2\frac{\pi^2}{4}\frac{c_v t}{H^2}\right], \quad (31)$$

$$c_v = \frac{\kappa}{S_s + \frac{\alpha^2}{K+(4/3)G}}, \quad (32)$$

where P is the normalized excess pore water pressure (−), U is the degree of consolidation (−), c_v is the consolidation coefficient ($m^2\ s^{-1}$), H is the sample height (m), κ is the hydraulic conductivity ($m\ s^{-1}$), S_s is the specific storage (m^{-1}), α is the Biot's coefficient (−), K is the bulk modulus (Pa) and G is the shear modulus (Pa).

We use 101 nodes and 100 elements to generate the simulation with the input data stated in Table 1. The proposed algorithm shows good performance indicated by a small error between numerical and analytical solutions (Figure 2). Furthermore, the mean absolute error for normalized excess pore water pressure at the dimensionless time t^* equal to 0.01,0.1,0.5 and 1 are 2.5×10^{-3},6.3×10^{-4},3.3×10^{-5} and 2.7×10^{-5}, respectively, with $t^* = \frac{c_v t}{H^2}$. The mean absolute error for the degree of consolidation also shows a small value of 3.9×10^{-3}.

3 | MODEL IMPLEMENTATION

To illustrate how MPeat works, we simulate peatland vertical growth with a fixed radius and flat substrate for 6,000 years using annual time steps. We assume that peat is an elastic material (Waddington et al., 2010), with fluid flow through pore space following Darcy's law. The substrate properties are impermeable and stiff, so at the base layer, the peat physical properties are not affected by compression of the substrate. In this model, the load is associated with a surficial peat addition (Equation 17) and plant weight (Equation 18), representing the natural condition of the peatland.

We run two groups of simulations based on annual air temperature and net rainfall with the parameter values summarized in Table 2. For the first group, we employ constant values for those two variables that are 6 ° C and 0.8 m $year^{-1}$, although this approach is not realistic, it gives baseline results and preliminary information to understand the model. Furthermore, this simplification is crucial for comparison purposes due to the high level of control of the model before proceeding to the next case. In the second group, we simulate the model using a more realistic climate, non-constant annual air temperature and net rainfall, developed from the sinusoidal function with some noise (Figure 3). We do not use the climate reconstruction model

TABLE 1 Input data for numerical and analytical solutions of Terzaghi's problem

Name	Symbol	Value	Unit
Load	q	1×10^5	Pa
Initial value of excess pore water pressure	p_{w0}	1×10^5	Pa
Young's modulus	E	1×10^8	Pa
Bulk modulus	K	5.56×10^7	Pa
Shear modulus	G	4.17×10^7	Pa
Hydraulic conductivity	κ	1×10^{-7}	$m\ s^{-1}$
Specific storage	S_s	1×10^{-5}	m^{-1}
Biot's coefficient	α	1	-
Sample height	H	1	m

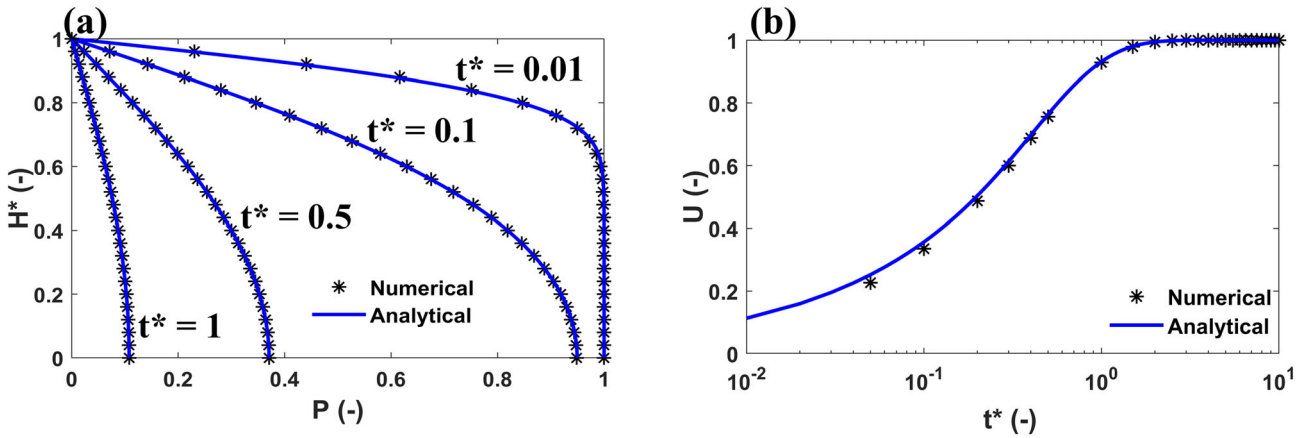

FIGURE 2 The comparison between numerical and analytical solutions of Terzaghi's problem. Normalized excess pore water pressure P with normalized height $H^* = y/H$ at various dimensionless time t^* (a) and degree of consolidation U with dimensionless time t^* (b)

TABLE 2 Symbols and parameter default values for the simulations

Name	Symbol	Value	Unit	Reference
Unsaturated zone decay rate	η_{un}	5×10^{-2}	$year^{-1}$	Clymo (1984)
Saturated zone decay rate	η_{sa}	8×10^{-5}	$year^{-1}$	Clymo (1984)
Biot's coefficient	α	1	–	Terzaghi (1943)
Bulk density initial value	ρ_0	50	$kg\ m^{-3}$	Lewis et al. (2012)
Carbon content	C	0.4	–	Loisel et al. (2014)
Active porosity initial value	ϕ_0	0.8	–	Quinton et al. (2000)
Bulk density and active porosity parameter	β	1	m^{-1}	Present study
Hydraulic conductivity initial value	κ_0	1×10^{-2}	$m\ s^{-1}$	Hoag and Price (1995)
Hydraulic conductivity parameter	ξ	15	–	Present study
Degree of saturation of water	S_w	0.4	–	Present study
Water retention empirical constant 1	λ	0.5	–	Present study
Water retention empirical constant 2	μ	0.4	m^{-1}	Present study
Specific storage	S_s	1.4×10^{-2}	m^{-1}	Hogan et al. (2006)
Specific weight of water	γ_w	9,800	$N\ m^{-3}$	Cheng (2020)
Peatland radius	l	500	m	Present study
Young's modulus parameter 1	χ	2×10^5	Pa	Present study
Young's modulus parameter 2	ζ	0.1	–	Present study
Shrub proportion	c_1	0.61	–	Moore et al. (2002)
Sedge or herb proportion	c_2	0.09	–	Moore et al. (2002)
Sphagnum proportion	c_3	0.3	–	Moore et al. (2002)
Shrub constant	d_1	0.4	–	Present study
Sedge or herb constant	d_2	0.4	–	Present study
Sphagnum constant	d_3	20	–	McNeil and Waddington (2003)
Gravitational acceleration	g	9.8	$m\ s^{-2}$	Present study

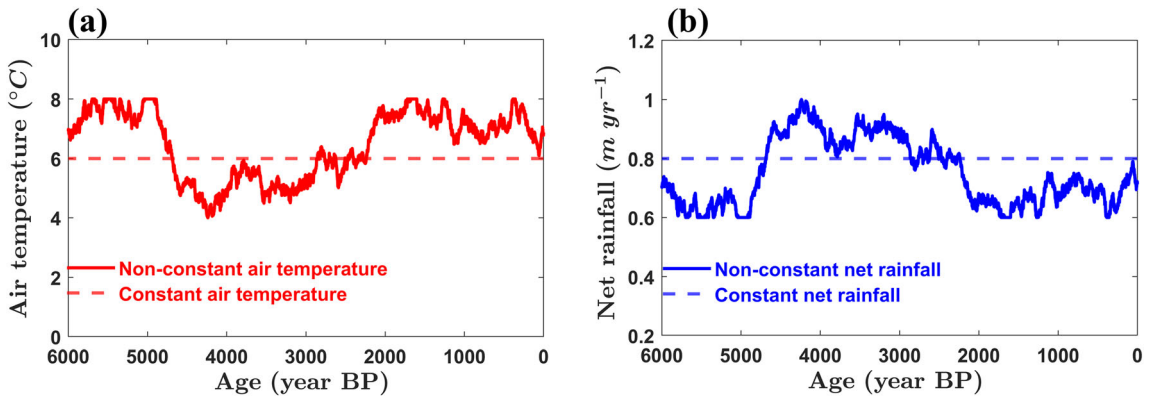

FIGURE 3 The constant and non-constant climate profile over 6,000 years. In the constant case, the value of air temperature (a) and net rainfall (b) are 6°C and 0.8 m yr^{-1}, while in the non-constant case, the value of air temperature and net rainfall ranging between 4°C - 8°C and 0.6 m yr^{-1}-1 m yr^{-1}

(e.g., Fischer & Jungclaus, 2011; Mauri et al., 2015; Pauling et al., 2006) because we want to keep it as simple as possible while also maintaining the effect of variable climate on the peatland growth over millennia.

We compare the simulation results of MPeat with DigiBog and HPM for peatland height, cumulative carbon and water table depth under constant and non-constant climate. DigiBog parameters are obtained from Morris et al. (2015) except for the unsaturated zone decay rate, saturated zone decay rate and initial bulk density, which are the same as MPeat values. HPM parameters, plant functional types and formulation, which includes the effect of air temperature, are obtained from Frolking et al. (2010) and Treat et al. (2013), with

the potential increase in bulk density $\Delta\rho$ is equal to 50 kg m^{-3}. For all three models, the cumulative carbon is formulated from cumulative organic mass multiplied by 40% of carbon content based on Loisel et al. (2014).

MPeat sensitivity analysis is conducted by changing the physical properties parameters of the model, that is, Young's modulus parameters χ and ζ and hydraulic conductivity parameter ξ. This is because field measurements of the Young's modulus and hydraulic conductivity of peat indicate that they have a wide range of values. We change the value of one parameter and all others remain the same as the baseline value (Table 2) for each simulation. Output variables examined from the sensitivity analysis include the value of bulk density, active porosity, hydraulic conductivity, Young's modulus, peatland height and cumulative carbon.

4 | SIMULATION RESULTS

4.1 | Group 1: Constant air temperature and net rainfall

The changes of peat physical properties with respect to depth (Figure 4) show that they have similar patterns that are a rapid shift around the depth of the water table, evolving to a relatively constant

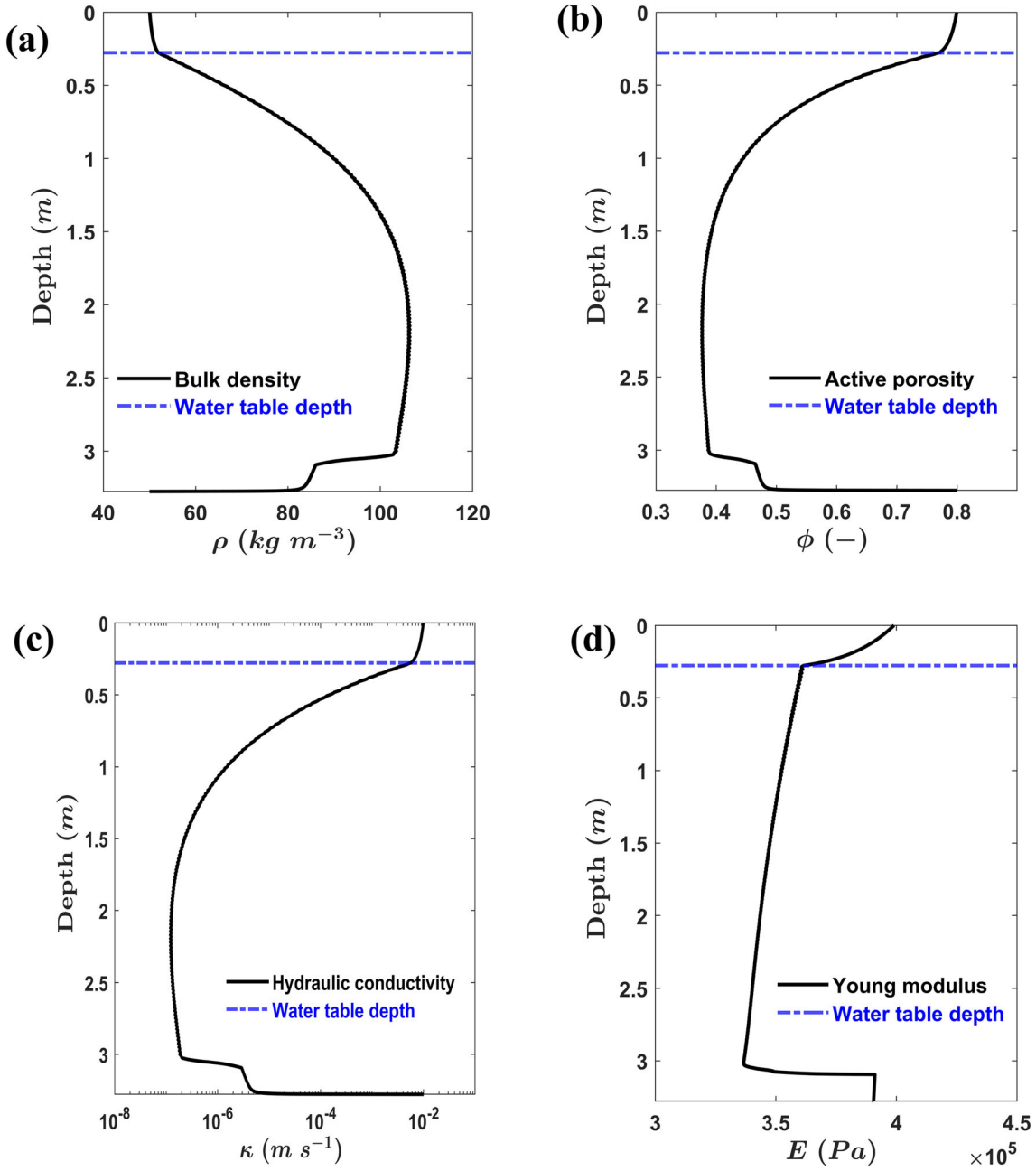

FIGURE 4 The profile of peat physical properties with depth, including bulk density (a), active porosity (b), hydraulic conductivity (c), and Young's modulus (d) after 6,000 simulated years under constant climate

value in the saturated zone. However, within the saturated zone, the trend changes abruptly at depths below 3 m due to the formation of the unsaturated zone about 400 years after peatland initiation (Figure 5c, MPeat). In particular, below 3 m, the bulk density value decreases dramatically while active porosity, hydraulic conductivity and Young's modulus values experienced a significant increase.

Comparison of MPeat to DigiBog and HPM (Figure 5) illustrates that all models produce similar long-term trends but with a number of key differences. After 6,000 years, peatland height estimated from MPeat (3.27 m) is lower than DigiBog (6.01 m) but relatively similar to HPM (3.25 m). MPeat simulates the highest cumulative carbon (123 kg C m^{-2}) compared to DigiBog (121 kg C m^{-2}) and HPM (120 kg C m^{-2}). MPeat also predicts the water table depth around 0.28 m in the final simulation year, while DigiBog and HPM predict around 0.39 and 0.29 m, respectively.

4.2 | Group 2: Non-constant air temperature and net rainfall

The fluctuations of air temperature and net rainfall provide a significant influence on the peat physical properties in the saturated zone. For example, the decrease in bulk density from 110 to 98 kg m^{-3} at a depth about 2.79 to 2.42 m (Figure 6a), and over the same interval, an increase in active porosity (Figure 6b) and hydraulic conductivity (Figure 6c) from approximately 0.36 to 0.41 and 7.34×10^{-8} to 3.82×10^{-7} m s^{-1}, respectively, corresponds to an abrupt shift to a cooler and wetter climatic interval around 5,000–4,200 years BP (Figure 3). The opposite patterns of bulk density, active porosity and hydraulic conductivity occur at a depth about 2.42 to 2.13 m due to a warmer and drier climatic interval around 4,200–3,600 years BP. The effect of climate change is less pronounced on Young's modulus due to its high fluctuations (Figure 6d). Young's modulus is controlled solely by the remaining mass, and peatland internal feedback mechanisms are likely to overwrite climate signal preservation contained in the remaining mass.

MPeat estimates lower peatland height than DigiBog (3.36 m vs. 5.99 m) but a greater peatland height than the HPM (3.36 m vs. 2.64 m) after 6,000 years (Figure 7a). MPeat simulates the highest cumulative carbon (131 kg C m^{-2}), compared to DigiBog (120 kg C m^{-2}) and HPM (98 kg C m^{-2}) (Figure 7b), which is similar to those of Group 1. The range of water table depths simulated by MPeat, DigiBog and HPM are 0.15 to 0.38 m, 0.22 to 0.67 m and 0.25 to 0.58 m, respectively, without including the initiation time

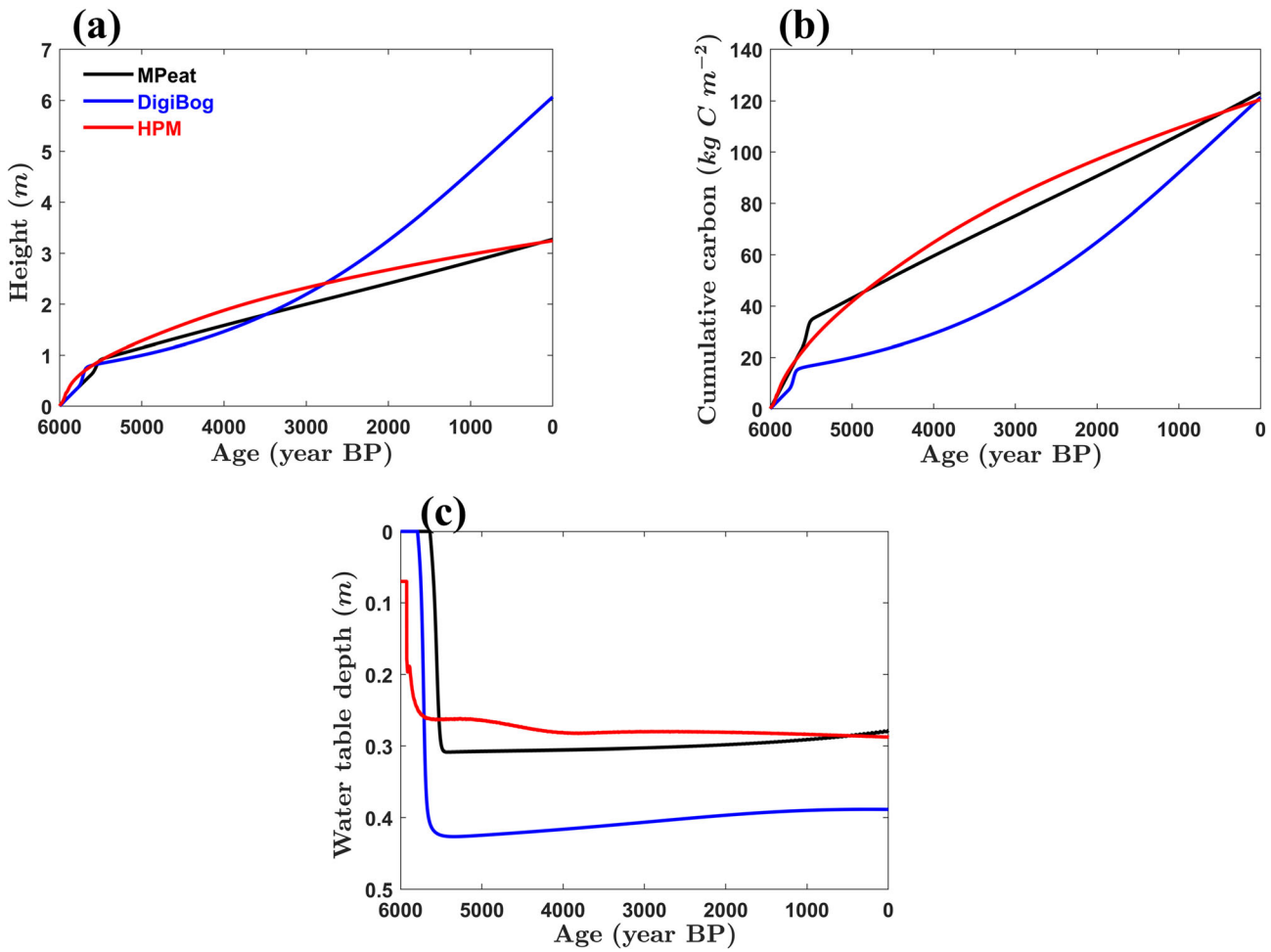

FIGURE 5 The comparison among MPeat, DigiBog, and HPM for peatland height (a), cumulative carbon (b), and water table depth (c) under constant climate

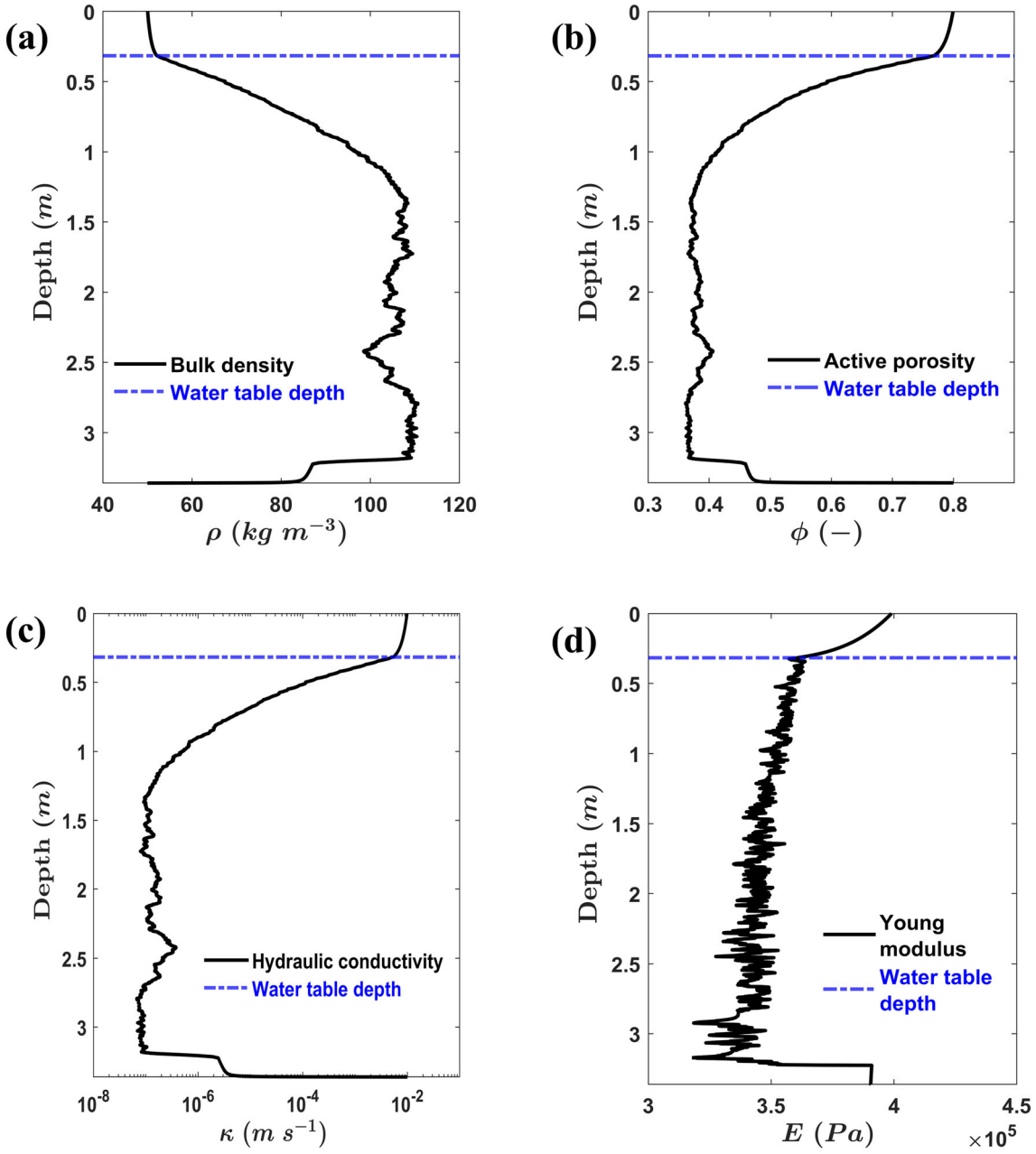

FIGURE 6 The profile of peat physical properties with depth, including bulk density (a), active porosity (b), hydraulic conductivity (c), and Young's modulus (d) after 6,000 simulated years under non-constant climate

when the unsaturated zone is not well developed (Figure 7c). Furthermore, water table depth simulated by DigiBog and HPM experiences sudden increases, particularly in the last 2,000 years, increases that are absent from the MPeat simulation.

4.3 | Sensitivity analysis

Changing Young's modulus parameters (χ and ζ, Equation 16) revealed that the other physical properties as well as peatland height and cumulative carbon are affected by the initial parameters that determine Young's modulus. Under constant climate (Figure 8), increasing the first Young's modulus parameter χ to 3×10^5 Pa resulted in a higher Young's modulus value to the range of $5 \times 10^5 - 6 \times 10^5$ Pa, which in turn reduced the bulk density to $50 - 81$ kg m^{-3} but increased the active porosity and hydraulic conductivity to interval $0.49 - 0.8$ and $6.65 \times 10^{-6} - 1 \times 10^{-2}$ m s^{-1}, respectively. A stiffer peat is less affected by compression, which leads to lower water retention due to higher hydraulic conductivity. Therefore, by increasing χ to 3×10^5 Pa, peatland height and cumulative carbon decreased by about 16% and 33% compared to the baseline value after 6,000 years (Figure 5, MPeat). On the other hand, increasing the second Young's modulus parameter ζ to 0.15 resulted in the lower Young's modulus ($3 \times 10^5 - 4 \times 10^5$ Pa) and consequently higher

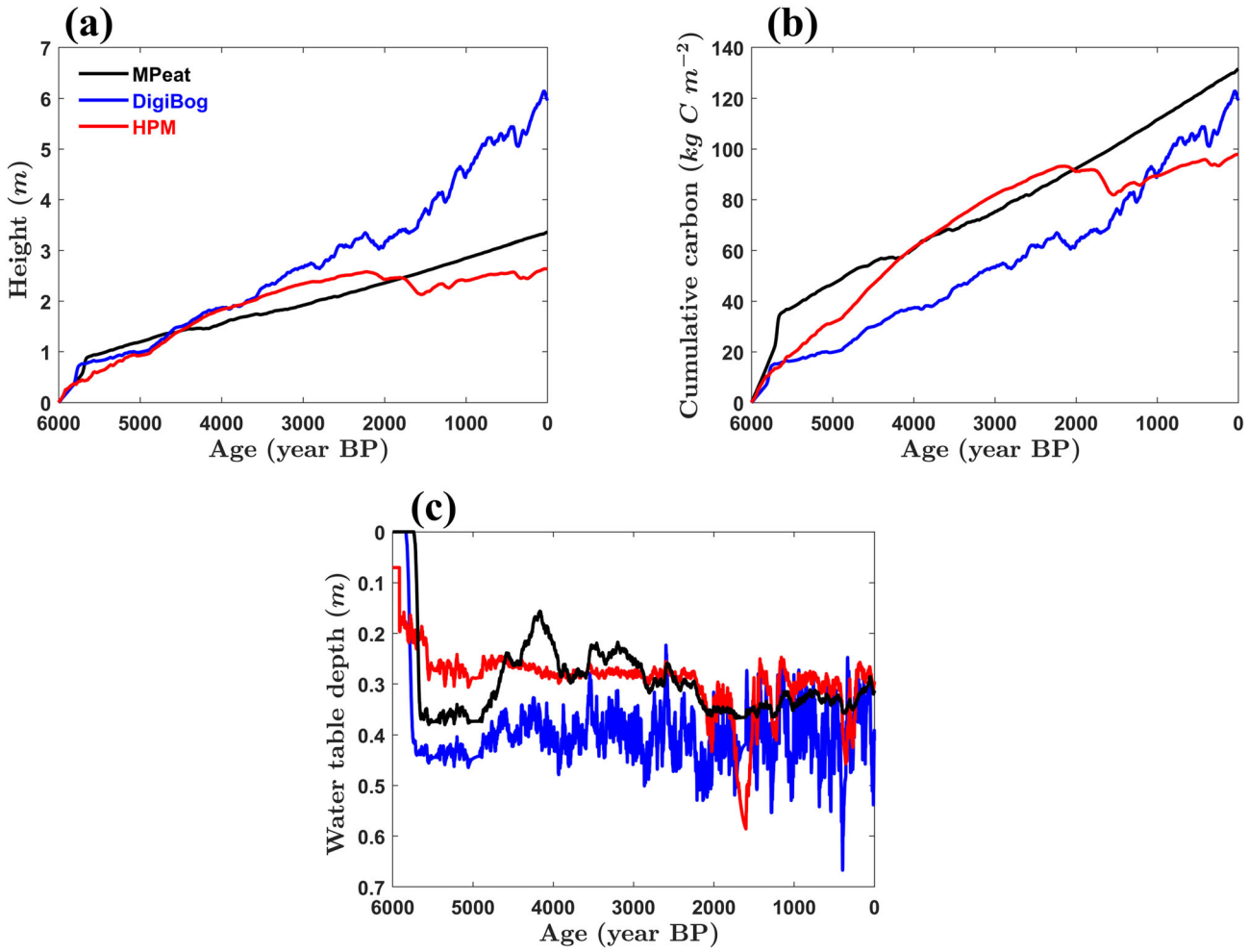

FIGURE 7 The comparison among MPeat, DigiBog, and HPM for peatland height (a), cumulative carbon (b), and water table depth (c) under non-constant climate

bulk density 50–111 kg m^{-3}) but lower active porosity (0.36–0.8) and hydraulic conductivity ($6.32 \times 10^{-8} - 1 \times 10^{-2}$ m s^{-1}). These conditions increased the peatland height and cumulative carbon by about 2% and 6% in the final simulation year.

Under non-constant climate (Figure 9), the influence of parameters χ and ζ on the output variables are similar to the constant climate case. Increasing χ to 3×10^5 Pa resulted in the lower bulk density (50–84 kg m^{-3}) but higher active porosity (0.47–0.8) and hydraulic conductivity ($4.04 \times 10^{-6} - 1 \times 10^{-2}$ m s^{-1}). As a consequence, peatland height and cumulative carbon were reduced by about 17% and 34% compared to the baseline value after 6,000 years (Figure 7, MPeat). Changing ζ to 0.15 increased bulk density (50–115 kg m^{-3}) but decreased active porosity (0.35–0.8) and hydraulic conductivity ($3.73 \times 10^{-8} - 1 \times 10^{-2}$ m s^{-1}), which in turn resulted in higher peatland (3.42 m) and cumulative carbon (139 kg C m^{-2}) after 6,000 years.

The hydraulic conductivity parameter (ξ, Equation 21) controls the decline of the hydraulic conductivity value as the active porosity becomes smaller due to the compression. Under constant climate, decreasing ξ to 12.5, which was associated with an increase in hydraulic conductivity value to the range of $8.80 \times 10^{-7} - 1 \times 10^{-2}$ m s^{-1}, reduced the peatland height by about 0.33 m and resulted in about 13 kg C m^{-2} lower cumulative carbon compared to the baseline value after 6,000 years. Under non-constant climate and ξ equal to 12.5, hydraulic conductivity increased to interval $5.28 \times 10^{-7} - 1 \times 10^{-2}$ m s^{-1}, which reduced peatland height and cumulative carbon by about 0.35 m and 14 kg C m^{-2} in the final simulation year. However, changing ξ had little impact on the other physical properties.

5 | DISCUSSION

Our results illustrate the influence of poroelastic deformation on the ecohydrological processes that lead to peat accumulation. As expected (Fenton, 1980; Quinton et al., 2000; Waddington et al., 2010; Whittington & Price, 2006), the most significant compaction in our model occurs at the transition from the unsaturated to the saturated zone. At this transition, peat experiences high effective stress due to unsaturated conditions. This results in the collapse of

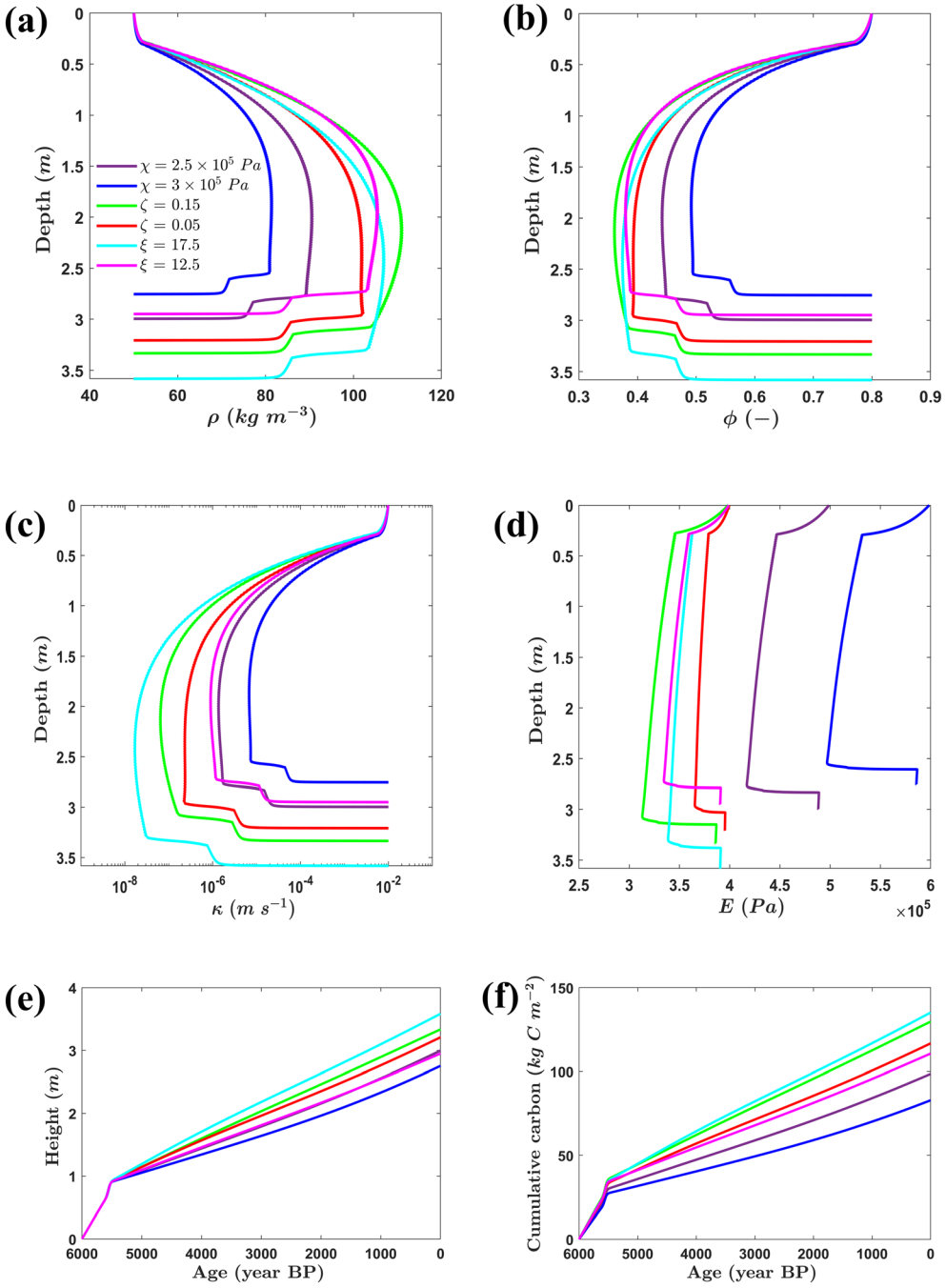

FIGURE 8 MPeat sensitivity analysis with the output variables including bulk density ρ (a), active porosity Φ (b), hydraulic conductivity κ (c), Young's modulus E (d), peatland height (e), and cumulative carbon (f) by changing the values of Young's modulus parameters χ and ζ, and hydraulic conductivity parameter ξ under constant climate. In the base runs (Figure 4 and Figure 5, MPeat) $\chi = 2 \times 10^5$ Pa, $\zeta = 0.1$, and $\xi = 15$

the pore structure, increasing bulk density and decreasing active porosity and hydraulic conductivity. The condition is different in the saturated zone where pore water pressure reduces the effective stress generating a relatively stable value of the physical properties (Figure 4a–c). This finding is in line with expectations and field measurement from Price (2003), who observes that effective stress decreases substantially below the water table.

Because most of the mechanical deformation occurs in the unsaturated zone, MPeat illustrates how water table depth has a considerable impact on the peat physical properties. During warming and drying climatic events, as depth to the water table increases, the value of bulk density increases and active porosity and hydraulic conductivity decline (Figure 6a–c). As observed in the field (Price et al., 2003), this mechanical behaviour acts to reduce water loss and increase drought resilience. In addition, compression also reduces peat volume, causing the peatland surface to drop. This drop in the peat surface acts to maintain the relative position of the water table, which in turn helps sustain PFTs associated with wet surface conditions (Schouten, 2002; Waddington et al., 2015). Conversely, a water surplus condition in the cooling and wetting period raises the water table, expands pore space and decreases effective stress. This condition reduces bulk density and increases active porosity and hydraulic conductivity, leading to lower water retention and raising drainage potential. Such variations in peat physical properties within the saturated

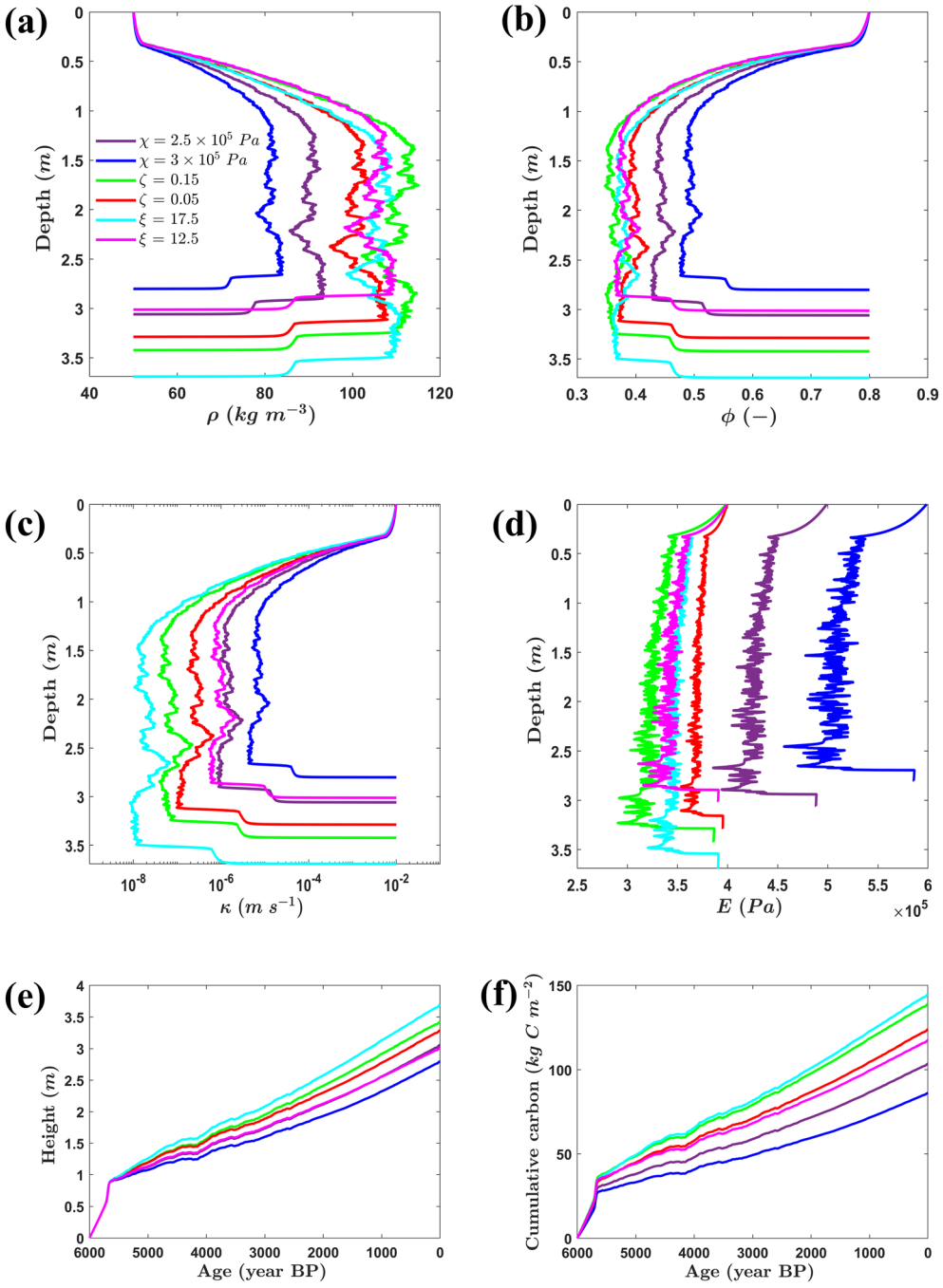

FIGURE 9 MPeat sensitivity analysis with the output variables including bulk density ρ (a), active porosity Φ (b), hydraulic conductivity κ (c), Young's modulus E (d), peatland height (e), and cumulative carbon (f) by changing the values of Young's modulus parameters χ and ζ, and hydraulic conductivity parameter ξ under non-constant climate. In the base runs (Figure 6 and Figure 7, MPeat) $\chi = 2 \times 10^5$ Pa, $\zeta = 0.1$, and $\xi = 15$

zone are routinely observed in cores and measured as dry bulk density. MPeat, therefore, has the capacity to model peat bulk density profiles in a way that can be compared to and complement other paleoclimatic indicators.

5.1 | Comparison to other ecohydrological models

MPeat, DigiBog and HPM provide similar long-term trends of peatland development, which indicates they are capable of describing the general evolution of a peatland, including the changes in height, cumulative carbon and water table depth. However, they have essential differences. The key difference between MPeat and Digibog is the absence of poroelasticity (Table 3). In effect, DigiBog models a stiff peat in which the unsaturated zone cannot deform. This absence of dynamic expansion and compaction have the greatest consequence under a variable climate, with DigiBog sustaining a thicker unsaturated zone and consequently greater peat thickness and less cumulative carbon (Figure 7). To some extent, these discrepancies can be reduced by adjusting the parameter values; however, as time progresses, the approach used in DigiBog will always tend to overestimate peatland height because it omits the effect of compression.

The difference between MPeat and HPM (Table 3) is somewhat less than with DigiBog, but this is primarily due to the empirical

relationship used to predict the change in bulk density as a function of remaining mass (Frolking et al., 2010). However, the HPM is also an inherently stiffer model and, as it evolves under a variable climate, tends to predict similar or deeper water tables than MPeat and consequently less cumulative carbon. The empirical relationships used by HPM, therefore, limit our understanding of mechanical feedback mechanisms.

A final point of difference between the three models is that under variable climate, the outputs from MPeat are smoother than either DigiBog or HPM (Figure 7). This smoothness is a consequence of the mechanical buffering inherent to the poroelastic response to changes in excess precipitation and illustrates the potential importance of mechanics in maintaining the resilience of peatland systems. These results are in agreement with a study from Nijp et al. (2017), indicating that the inclusion of moss water storage and peat volume change because of mechanical deformation increase the projection of peatland drought resilience.

It can therefore be concluded that mechanical process plays a vital role in the peatland carbon stock (Figure 10). Compression provides negative feedback to an increasing water table depth (Waddington et al., 2015), which leads to the shorter residence time of plant litter in the unsaturated zone, increasing rates of carbon burial and reducing CO_2 emissions. The experiment from Blodau et al. (2004) corroborates this view and indicates that the production rate of CO_2 rises substantially with an increasing water table depth.

TABLE 3 The differences in approach for modelling peat physical properties among MPeat, DigiBog and HPM

MPeat	DigiBog	HPM
Bulk density is a function of fluid flow and solid deformation.	Bulk density is a constant.	Bulk density is a function of remaining mass.
Active porosity is a function of fluid flow and solid deformation.	Drainable porosity is a constant.	Porosity is a function of peat bulk density and particle bulk density of organic matter.
Hydraulic conductivity is a function of active porosity.	Hydraulic conductivity is a function of remaining mass.	Hydraulic conductivity is a function of peat bulk density.
Young's modulus is a function of remaining mass.	-	-

5.2 | Comparison with field measurement

A considerable uncertainty in the MPeat model is Young's modulus which in turn has the ability to influence the other physical properties as shown in the sensitivity analysis. Values of Young's modulus of peat are hard to measure in situ, and laboratory-determined values are of questionable applicability in the field. For example, Dykes (2008) measured Young's modulus of Irish peat and obtained values ranging from 1.15×10^3 to 3.5×10^3 Pa and concluded that these very low values might be correlated with sample preparation that affected the strain measurement. As MPeat simulations evolve, Young's modulus values ranging between 2.9×10^5 and 6×10^5 Pa are far higher than the values provided by Dykes (2008). Nonetheless, according to Mesri and Ajlouni (2007), the ratio between Young's modulus with undrained shear strength lies in the range 20–80, and the reported data for undrained shear strength is in the range of $4 \times 10^3 - 2 \times 10^4$ Pa, depending on the degree of humification and water content (Boylan et al., 2008; Long, 2005). Therefore, the plausible range of peat Young's modulus is $8 \times 10^4 - 1.6 \times 10^6$ Pa, the range

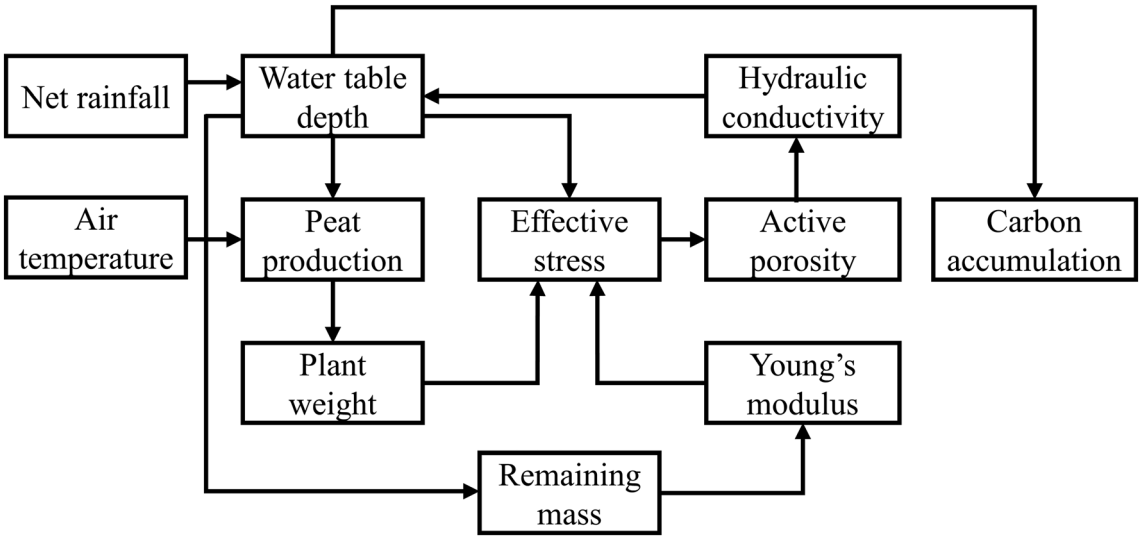

FIGURE 10 Overview of the influence of mechanics on peatland ecohydrology and carbon stock resilience to the external perturbations, including the changes in net rainfall and air temperature

value that is used in MPeat. As to the effect of decay on the Young's modulus of peat, this remains unknown beyond the expectation that decay should reduce elasticity within the range of reported values.

Some reassurance that the initial values of Young's modulus chosen in MPeat and subsequent values generated via decay are reasonable come from the comparison of the range of modelled and observed physical properties. Reported measurements of active porosity decrease with depth from as high as 0.8 near the top of the unsaturated zone to as low as 0.1 in the saturated zone (Hoag & Price, 1997; Quinton et al., 2000; Quinton et al., 2008; Siegel et al., 1995), similar to the MPeat active porosity pattern and values that range from 0.8 in the unsaturated zone to 0.34 in the saturated zone. Dry bulk density and hydraulic conductivity calculated in MPeat are between 50–115 kg m^{-3} and $8.42 \times 10^{-9} - 1 \times 10^{-2}$ m s^{-1} broadly in line with reported measurements of dry bulk density and hydraulic conductivity around 30–120 kg m^{-3} and $7 \times 10^{-9} - 1.6 \times 10^{-2}$ m s^{-1} (Clymo, 1984, 2004; Fraser et al., 2001; Hoag & Price, 1995; Hogan et al., 2006). Moreover, a considerable increase of hydraulic conductivity at the base of the peat profile obtained from MPeat, corresponding to peat accumulation under fully saturated conditions, is similar to some field observations (Clymo, 2004; Kneale, 1987; Waddington & Roulet, 1997). However, a notable difference between the modelled and measured peat physical properties is that the range of dry bulk densities generated by MPeat in the saturated zone is narrower than the range typically observed in many peat deposits. The most likely explanation for this is the constant initial value of Young's modulus, which in reality will vary depending on PFT, with woody stemmed shrubs having a greater initial value than moss.

5.3 | Model limitations and future developments

In one dimension, an alternative formulation that could address the limited range in dry bulk density would be to couple Young's modulus to PFT, shrub having a higher Young's modulus and *Sphagnum* a lower Young's modulus. This process requires a more generic peat production model that could be altered according to PFT, for example, the generalization of two-dimensional asymmetric Gaussian function from Frolking et al. (2010). In turn, the coupling between Young's modulus and PFT would generate a critical drying threshold below which shrub would become dominant, increasing stiffness in the peat and potentially acting as a positive feedback increasing carbon emissions and reducing the rate of carbon accumulation. Potentially, this could be a natural threshold or tipping point in peatland evolution.

The effect of belowground structure, including shoots and roots of the vascular plants, could provide a supporting matrix that reduces the compression effect in the unsaturated zone (Malmer et al., 1994). This could be implemented in MPeat through Young's modulus equation which determines the ability of the peat to withstand compression. However, this process would increase model uncertainties because of the increasing number of free parameters. Therefore, a more complete sensitivity analysis that considers the interaction between parameters (e.g., Quillet et al., 2013) would be helpful for the future development of the MPeat.

In one dimension, MPeat cannot capture the spatial variability of peat physical properties and thickness in a horizontal direction, yet many physical properties vary in two or three dimensions. For example, as shown by Lewis et al. (2012), the bulk density and hydraulic conductivity differ systematically between the centre of a peatland and its margin. Higher dry bulk densities and lower hydraulic conductivities at the margins help peatland to hold the water and promote greater peat accumulation (Lapen et al., 2005). To understand these processes, it should be possible to extend MPeat into two or three dimensions. However, this extension is challenging because it increases the model complexities and becomes computationally expensive in terms of model run times. To achieve this, simplifying assumptions may be required, including turning off component parts of the model and exploring the mechanical behaviour of different bilayer peatland geometries. The approach should have considerable potential at improving our understanding of peat failure (mass movement), pipe formation and whether patterned pool systems have a mechanical origin. Indeed, the thresholds for mechanical failure of peat are also natural limits to carbon accumulation in a landscape and are tipping points for a notable natural hazard (Crisp et al., 1964; McCahon et al., 1987; Warburton et al., 2003).

Finally, another aspect that could be developed to produce a more plausible peatland growth model is the presence of gas bubbles. The entrapped gas bubbles block the pore space and affect the water flow, thus decreasing hydraulic conductivity (Baird & Waldron, 2003; Beckwith & Baird, 2001; Reynolds et al., 1992). Besides that, they have been shown to provide a noticeable effect on pore water pressure (Kellner et al., 2004), which in turn could influence effective stress. Introducing this aspect into the model requires a deep understanding of a complex peat pore structure, including the effect of dual-porosity, to determine the area where bubbles get trapped.

6 | CONCLUSION

MPeat is developed based on interactions among mechanical, ecological and hydrological processes that are theoretically reasonable and empirically proven to occur in the real peatland. These interactions influence peat physical properties, such as bulk density, active porosity, hydraulic conductivity and Young's modulus through the coupling between fluid flow and solid deformation, which becomes the core of the model. MPeat illustrates the important function of poroelasticity in enhancing peatland resilience and sustaining peatland carbon stock in the face of climate change. The insights gained from this model may be of assistance to understand the long-term impact of climate change on the global carbon balance and the natural mechanical limits to peatland accumulation.

ACKNOWLEDGEMENTS

We would like to thank Andy Baird and Nigel Roulet for interesting discussions on an earlier version of the model. This work was funded

by the Directorate General of Higher Education (DIKTI) Indonesia, PhD scholarship awarded to AWM. We also thank Andy Reeve, Paul Morris and anonymous reviewers for their insightful and constructive comments.

CONFLICT OF INTEREST

The authors declare no conflict of interest.

DATA AVAILABILITY STATEMENT

The codes that support the findings of this study are openly available in zenodo at https://doi.org/10.5281/zenodo.4786346 (Mahdiyasa, 2021).

ORCID

Adilan W. Mahdiyasa https://orcid.org/0000-0002-9940-3920
David J. Large https://orcid.org/0000-0003-0559-8526
Bagus P. Muljadi https://orcid.org/0000-0001-7318-0856
Matteo Icardi https://orcid.org/0000-0003-3924-3117
Savvas Triantafyllou https://orcid.org/0000-0001-7038-0756

REFERENCES

Baird, A. J., Morris, P. J., & Belyea, L. R. (2012). The DigiBog peatland development model 1: Rationale, conceptual model, and hydrological basis. *Ecohydrology*, *5*(3), 242–255. https://doi.org/10.1002/eco.230

Baird, A. J., & Waldron, S. (2003). Shallow horizontal groundwater flow in peatlands is reduced by bacteriogenic gas production. *Geophysical Research Letters*, *30*(20), 1–4. https://doi.org/10.1029/2003GL018233

Ballard, C. E., McIntyre, N., Wheater, H. S., Holden, J., & Wallage, Z. E. (2011). Hydrological modelling of drained blanket peatland. *Journal of Hydrology*, *407*(1), 81–93. https://doi.org/10.1016/j.jhydrol.2011.07.005

Beckwith, C. W., & Baird, A. J. (2001). Effect of biogenic gas bubbles on water flow through poorly decomposed blanket peat. *Water Resources Research*, *37*(3), 551–558. https://doi.org/10.1029/2000WR900303

Belyea, L. R. (2009). Nonlinear dynamics of peatlands and potential feedbacks on the climate system. In A. J. Baird, L. R. Belyea, X. Comas, A. Reeve, & L. D. Slater (Eds.), *Carbon cycling in northern peatlands* (pp. 5–18). American Geophysical Union. https://doi.org/10.1029/2008GM000829

Belyea, L. R., & Baird, A. J. (2006). Beyond the "limits to peat bog growth": Cross-scale feedback in peatland development. *Ecological Monographs*, *76*(3), 299–322. https://doi.org/10.1890/0012-9615(2006)076%5B0299:BTLTPB%5D2.0.CO;2

Belyea, L. R., & Clymo, R. S. (2001). Feedback control of the rate of peat formation. *Proceedings of the Royal Society of London. Series B: Biological Sciences*, *268*(1473), 1315–1321. https://doi.org/10.1098/rspb.2001.1665

Biot, M. A. (1941). General theory of three-dimensional consolidation. *Journal of Applied Physics*, *12*(2), 155–164. https://doi.org/10.1063/1.1712886

Blodau, C., Basiliko, N., & Moore, T. R. (2004). Carbon turnover in peatland mesocosms exposed to different water table levels. *Biogeochemistry*, *67*(3), 331–351. https://doi.org/10.1023/B:BIOG.0000015788.30164.e2

Boylan, N., Jennings, P., & Long, M. (2008). Peat slope failure in Ireland. *Quarterly Journal of Engineering Geology and Hydrogeology*, *41*(1), 93–108. https://doi.org/10.1144/1470-9236/06-028

Cheng, A. H. D. (2020). A linear constitutive model for unsaturated poroelasticity by micromechanical analysis. *International Journal for Numerical and Analytical Methods in Geomechanics*, *44*(4), 455–483. https://doi.org/10.1002/nag.3033

Childs, E. C. (1969). *An introduction to the physical basis of soil water phenomena*. John Wiley & Sons Ltd.

Clymo, R. S. (1984). The limits to peat bog growth. *Philosophical Transactions of the Royal Society of London. B, Biological Sciences*, *303*(1117), 605–654. https://doi.org/10.1098/rstb.1984.0002

Clymo, R. S. (2004). Hydraulic conductivity of peat at Ellergower Moss, Scotland. *Hydrological Processes*, *18*(2), 261–274. https://doi.org/10.1002/hyp.1374

Crisp, D. T., Rawes, M., & Welch, D. (1964). A Pennine peat slide. *The Geographical Journal*, *130*(4), 519–524. https://doi.org/10.2307/1792263

Dykes, A. P. (2008). Tensile strength of peat: Laboratory measurement and role in Irish blanket bog failures. *Landslides*, *5*(4), 417–429. https://doi.org/10.1007/s10346-008-0136-1

Fenton, J. H. C. (1980). The rate of peat accumulation in Antarctic Moss banks. *Journal of Ecology*, *68*(1), 211–228. https://doi.org/10.2307/2259252

Fischer, N., & Jungclaus, J. H. (2011). Evolution of the seasonal temperature cycle in a transient Holocene simulation: Orbital forcing and sea-ice. *Climate of the Past*, *7*(4), 1139–1148. https://doi.org/10.5194/cp-7-1139-2011

Fraser, C. J. D., Roulet, N. T., & Moore, T. R. (2001). Hydrology and dissolved organic carbon biogeochemistry in an ombrotrophic bog. *Hydrological Processes*, *15*(16), 3151–3166. https://doi.org/10.1002/hyp.322

Frolking, S., Roulet, N. T., Tuittila, E., Bubier, J. L., Quillet, A., Talbot, J., & Richard, P. J. H. (2010). A new model of Holocene peatland net primary production, decomposition, water balance, and peat accumulation. *Earth System Dynamics*, *1*(1), 1–21. https://doi.org/10.5194/esd-1-1-2010

Glaser, P. H., Chanton, J. P., Morin, P., Rosenberry, D. O., Siegel, D. I., Ruud, O., Chasar, L. I., & Reeve, A. S. (2004). Surface deformations as indicators of deep ebullition fluxes in a large northern peatland. *Global Biogeochemical Cycles*, *18*(1), 1–15. https://doi.org/10.1029/2003GB002069

Green, D. H., & Wang, H. F. (1990). Specific storage as a poroelastic coefficient. *Water Resources Research*, *26*(7), 1631–1637. https://doi.org/10.1029/WR026i007p01631

Hanrahan, E. T. (1954). An investigation of some physical properties of peat. *Géotechnique*, *4*(3), 108–123. https://doi.org/10.1680/geot.1954.4.3.108

Heinemeyer, A., Croft, S., Garnett, M. H., Gloor, E., Holden, J., Lomas, M. R., & Ineson, P. (2010). The MILLENNIA peat cohort model, predicting past, present and future soil carbon budgets and fluxes under changing climates in peatlands. *Climate Research*, *45*(1), 207–226. https://doi.org/10.3354/cr00928

Hilbert, D. W., Roulet, N., & Moore, T. (2000). Modelling and analysis of peatlands as dynamical systems. *Journal of Ecology*, *88*(2), 230–242. https://doi.org/10.1046/j.1365-2745.2000.00438.x

Hoag, R. S., & Price, J. S. (1995). A field-scale, natural gradient solute transport experiment in peat at a Newfoundland blanket bog. *Journal of Hydrology*, *172*(1), 171–184. https://doi.org/10.1016/0022-1694(95)02696-M

Hoag, R. S., & Price, J. S. (1997). The effects of matrix diffusion on solute transport and retardation in undisturbed peat in laboratory columns. *Journal of Contaminant Hydrology*, *28*(3), 193–205. https://doi.org/10.1016/S0169-7722(96)00085-X

Hobbs, N. B. (1986). Mire morphology and the properties and behaviour of some British and foreign peats. *Quarterly Journal of Engineering Geology and Hydrogeology*, *19*(1), 7–80. https://doi.org/10.1144/gsl.Qjeg.1986.019.01.02

Hobbs, N. B. (1987). A note on the classification of peat. *Géotechnique*, *37*(3), 405–407. https://doi.org/10.1680/geot.1987.37.3.405

Hogan, J. M., van der Kamp, G., Barbour, S. L., & Schmidt, R. (2006). Field methods for measuring hydraulic properties of peat deposits. *Hydrological Processes*, *20*(17), 3635–3649. https://doi.org/10.1002/hyp.6379

Ingram, H. A. P. (1982). Size and shape in raised mire ecosystems: A geophysical model. *Nature*, *297*(5864), 300–303. https://doi.org/10.1038/297300a0

Ise, T., Dunn, A. L., Wofsy, S. C., & Moorcroft, P. R. (2008). High sensitivity of peat decomposition to climate change through water-table feedback. *Nature Geoscience*, *1*(11), 763–766. https://doi.org/10.1038/ngeo331

Jackson, R. B., Lajtha, K., Crow, S. E., Hugelius, G., Kramer, M. G., & Piñeiro, G. (2017). The ecology of soil carbon: Pools, vulnerabilities, and biotic and abiotic controls. *Annual Review of Ecology, Evolution, and Systematics*, *48*(1), 419–445. https://doi.org/10.1146/annurev-ecolsys-112414-054234

Kellner, E., Price, J. S., & Waddington, J. M. (2004). Pressure variations in peat as a result of gas bubble dynamics. *Hydrological Processes*, *18*(13), 2599–2605. https://doi.org/10.1002/hyp.5650

Kneale, P. E. (1987). Sensitivity of the groundwater mound model for predicting mire topography. *Hydrology Research*, *18*(4–5), 193–202. https://doi.org/10.2166/nh.1987.0014

Lapen, D. R., Price, J. S., & Gilbert, R. (2005). Modelling two-dimensional steady-state groundwater flow and flow sensitivity to boundary conditions in blanket peat complexes. *Hydrological Processes*, *19*(2), 371–386. https://doi.org/10.1002/hyp.1507

Lewis, C., Albertson, J., Xu, X., & Kiely, G. (2012). Spatial variability of hydraulic conductivity and bulk density along a blanket peatland hillslope. *Hydrological Processes*, *26*(10), 1527–1537. https://doi.org/10.1002/hyp.8252

Loisel, J., van Bellen, S., Pelletier, L., Talbot, J., Hugelius, G., Karran, D., Yu, Z., Nichols, J., & Holmquist, J. (2017). Insights and issues with estimating northern peatland carbon stocks and fluxes since the Last Glacial Maximum. *Earth-Science Reviews*, *165*, 59–80. https://doi.org/10.1016/j.earscirev.2016.12.001

Loisel, J., Yu, Z., Beilman, D. W., Camill, P., Alm, J., Amesbury, M. J., Anderson, D., Andersson, S., Bochicchio, C., Barber, K., Belyea, L. R., Bunbury, J., Chambers, F. M., Charman, D. J., de Vleeschouwer, F., Fiałkiewicz-Kozieł, B., Finkelstein, S. A., Gałka, M., Garneau, M., … Zhou, W. (2014). A database and synthesis of northern peatland soil properties and Holocene carbon and nitrogen accumulation. *The Holocene*, *24*(9), 1028–1042. https://doi.org/10.1177/0959683614538073

Long, M. (2005). Review of peat strength, peat characterisation and constitutive modelling of peat with reference to landslides. *Studia Geotechnica et Mechanica*, *27*(3–4), 67–90.

Lunt, P. H., Fyfe, R. M., & Tappin, A. D. (2019). Role of recent climate change on carbon sequestration in peatland systems. *Science of the Total Environment*, *667*, 348–358. https://doi.org/10.1016/j.scitotenv.2019.02.239

Mahdiyasa, A. W. (2021). MPeat 1.0. Zenodo. https://doi.org/10.5281/zenodo.4786346

Malmer, N., Svensson, B. M., & Wallén, B. (1994). Interactions between Sphagnum mosses and field layer vascular plants in the development of peat-forming systems. *Folia Geobotanica & Phytotaxonomica*, *29*(4), 483–496. https://doi.org/10.1007/BF02883146

Mauri, A., Davis, B. A. S., Collins, P. M., & Kaplan, J. O. (2015). The climate of Europe during the Holocene: A gridded pollen-based reconstruction and its multi-proxy evaluation. *Quaternary Science Reviews*, *112*, 109–127. https://doi.org/10.1016/j.quascirev.2015.01.013

McCahon, C. P., Carling, P. A., & Pascoe, D. (1987). Chemical and ecological effects of a Pennine peat-slide. *Environmental Pollution*, *45*(4), 275–289. https://doi.org/10.1016/0269-7491(87)90102-3

McNeil, P., & Waddington, J. M. (2003). Moisture controls on Sphagnum growth and CO2 exchange on a cutover bog. *Journal of Applied Ecology*, *40*(2), 354–367. https://doi.org/10.1046/j.1365-2664.2003.00790.x

Mesri, G., & Ajlouni, M. (2007). Engineering properties of fibrous peats. *Journal of Geotechnical and Geoenvironmental Engineering*, *133*(7), 850–866. https://doi.org/10.1061/(ASCE)1090-0241(2007)133:7(850)

Moore, T. R., Bubier, J. L., Frolking, S. E., Lafleur, P. M., & Roulet, N. T. (2002). Plant biomass and production and CO2 exchange in an ombrotrophic bog. *Journal of Ecology*, *90*(1), 25–36. https://doi.org/10.1046/j.0022-0477.2001.00633.x

Moore, T. R., Trofymow, J. A., Siltanen, M., Prescott, C., & CIDET Working Group. (2005). Patterns of decomposition and carbon, nitrogen, and phosphorus dynamics of litter in upland forest and peatland sites in Central Canada. *Canadian Journal of Forest Research*, *35*(1), 133–142. https://doi.org/10.1139/x04-149

Morris, P. J., Baird, A. J., & Belyea, L. R. (2012). The DigiBog peatland development model 2: Ecohydrological simulations in 2D. *Ecohydrology*, *5*(3), 256–268. https://doi.org/10.1002/eco.229

Morris, P. J., Baird, A. J., Young, D. M., & Swindles, G. T. (2015). Untangling climate signals from autogenic changes in long-term peatland development. *Geophysical Research Letters*, *42*(24), 10,788–710,797. https://doi.org/10.1002/2015GL066824

Morris, P. J., Belyea, L. R., & Baird, A. J. (2011). Ecohydrological feedbacks in peatland development: A theoretical modelling study. *Journal of Ecology*, *99*(5), 1190–1201. https://doi.org/10.1111/j.1365-2745.2011.01842.x

Nijp, J. J., Metselaar, K., Limpens, J., Teutschbein, C., Peichl, M., Nilsson, M. B., Berendse, F., & van der Zee, S. E. A. T. M. (2017). Including hydrological self-regulating processes in peatland models: Effects on peatmoss drought projections. *Science of the Total Environment*, *580*, 1389–1400. https://doi.org/10.1016/j.scitotenv.2016.12.104

Pauling, A., Luterbacher, J., Casty, C., & Wanner, H. (2006). Five hundred years of gridded high-resolution precipitation reconstructions over Europe and the connection to large-scale circulation. *Climate Dynamics*, *26*(4), 387–405. https://doi.org/10.1007/s00382-005-0090-8

Price, J. S. (2003). Role and character of seasonal peat soil deformation on the hydrology of undisturbed and cutover peatlands. *Water Resources Research*, *39*(9), 1–10. https://doi.org/10.1029/2002WR001302

Price, J. S., Heathwaite, A. L., & Baird, A. J. (2003). Hydrological processes in abandoned and restored peatlands: An overview of management approaches. *Wetlands Ecology and Management*, *11*(1), 65–83. https://doi.org/10.1023/A:1022046409485

Quillet, A., Frolking, S., Garneau, M., Talbot, J., & Peng, C. (2013). Assessing the role of parameter interactions in the sensitivity analysis of a model of peatland dynamics. *Ecological Modelling*, *248*, 30–40. https://doi.org/10.1016/j.ecolmodel.2012.08.023

Quinton, W. L., Gray, D. M., & Marsh, P. (2000). Subsurface drainage from hummock-covered hillslopes in the Arctic tundra. *Journal of Hydrology*, *237*(1), 113–125. https://doi.org/10.1016/S0022-1694(00)00304-8

Quinton, W. L., Hayashi, M., & Carey, S. K. (2008). Peat hydraulic conductivity in cold regions and its relation to pore size and geometry. *Hydrological Processes*, *22*(15), 2829–2837. https://doi.org/10.1002/hyp.7027

Reeve, A. S., Glaser, P. H., & Rosenberry, D. O. (2013). Seasonal changes in peatland surface elevation recorded at GPS stations in the red Lake Peatlands, northern Minnesota, USA. *Journal of Geophysical Research: Biogeosciences*, *118*(4), 1616–1626. https://doi.org/10.1002/2013JG002404

Reynolds, W. D., Brown, D. A., Mathur, S. P., & Overend, R. P. (1992). Effect of in-situ gas accumulation on the hydraulic conductivity of peat. *Soil Science*, *153*(5), 397–408.

Schouten, M. G. C. (2002). *Conservation and restoration of raised bogs: Geological, hydrological, and ecological studies*. The Government Stationary Office.

Siegel, D. I., Reeve, A. S., Glaser, P. H., & Romanowicz, E. A. (1995). Climate-driven flushing of pore water in peatlands. *Nature*, *374*(6522), 531–533. https://doi.org/10.1038/374531a0

Swindles, G. T., Morris, P. J., Baird, A. J., Blaauw, M., & Plunkett, G. (2012). Ecohydrological feedbacks confound peat-based climate reconstructions. *Geophysical Research Letters*, *39*(11), 1–4. https://doi.org/10.1029/2012GL051500

Swinnen, W., Broothaerts, N., & Verstraeten, G. (2019). Modelling long-term blanket peatland development in eastern Scotland. *Biogeosciences*, *16*(20), 3977–3996. https://doi.org/10.5194/bg-16-3977-2019

Terzaghi, K. (1943). *Theoretical soil mechanics*. John Wiley & Sons, Inc. https://doi.org/10.1002/9780470172766

Treat, C. C., Wisser, D., Marchenko, S., & Frolking, S. (2013). Modelling the effects of climate change and disturbance on permafrost stability in northern organic soil. *Mires and Peat*, *12*, 1–17.

Verruijt, A. (2018). Numerical and analytical solutions of poroelastic problems. *Geotechnical Research*, *5*(1), 39–50. https://doi.org/10.1680/jgere.15.00006

Waddington, J. M., Kellner, E., Strack, M., & Price, J. S. (2010). Differential peat deformation, compressibility, and water storage between peatland microforms: Implications for ecosystem function and development. *Water Resources Research*, *46*(7), 1–12. https://doi.org/10.1029/2009WR008802

Waddington, J. M., Morris, P. J., Kettridge, N., Granath, G., Thompson, D. K., & Moore, P. A. (2015). Hydrological feedbacks in northern peatlands. *Ecohydrology*, *8*(1), 113–127. https://doi.org/10.1002/eco.1493

Waddington, J. M., & Roulet, N. T. (1997). Groundwater flow and dissolved carbon movement in a boreal peatland. *Journal of Hydrology*, *191*(1), 122–138. https://doi.org/10.1016/S0022-1694(96)03075-2

Wang, H. F. (2000). *Theory of linear poroelasticity with applications to geomechanics and hydrogeology*. Princeton University Press.

Warburton, J., Higgitt, D., & Mills, A. (2003). Anatomy of a Pennine peat slide, Northern England. *Earth Surface Processes and Landforms*, *28*(5), 457–473. https://doi.org/10.1002/esp.452

Whittington, P. N., & Price, J. S. (2006). The effects of water table drawdown (as a surrogate for climate change) on the hydrology of a fen peatland, Canada. *Hydrological Processes*, *20*(17), 3589–3600. https://doi.org/10.1002/hyp.6376

Young, D. M., Baird, A. J., Morris, P. J., & Holden, J. (2017). Simulating the long-term impacts of drainage and restoration on the ecohydrology of peatlands. *Water Resources Research*, *53*(8), 6510–6522. https://doi.org/10.1002/2016WR019898

Yu, Z., Campbell, I. D., Vitt, D. H., & Apps, M. J. (2001). Modelling long-term peatland dynamics. I. Concepts, review, and proposed design. *Ecological Modelling*, *145*(2), 197–210. https://doi.org/10.1016/S0304-3800(01)00391-X

Yu, Z., Loisel, J., Brosseau, D. P., Beilman, D. W., & Hunt, S. J. (2010). Global peatland dynamics since the Last Glacial Maximum. *Geophysical Research Letters*, *37*(13), 1–5. https://doi.org/10.1029/2010GL043584

Zhu, J., Wang, Y., Wang, Y., Mao, Z., & Langendoen, E. J. (2020). How does root biodegradation after plant felling change root reinforcement to soil? *Plant and Soil*, *446*(1), 211–227. https://doi.org/10.1007/s11104-019-04345-x

Zienkiewicz, O. C., Taylor, R. L., & Zhu, J. Z. (2013). *The finite element method: Its basis and fundamentals* (7th ed.). Elsevier.

How to cite this article: Mahdiyasa, A. W., Large, D. J., Muljadi, B. P., Icardi, M., & Triantafyllou, S. (2021). MPeat—A fully coupled mechanical-ecohydrological model of peatland development. *Ecohydrology*, e2361. https://doi.org/10.1002/eco.2361